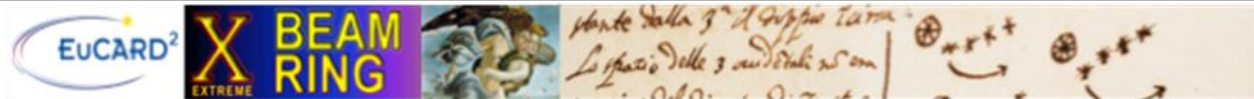


Diagnostics with undulator radiation

Sara Casalbuoni

ANKA, Karlsruhe Institute of Technology, Karlsruhe, Germany

ANKA



Beam Dynamics
meets Diagnostics

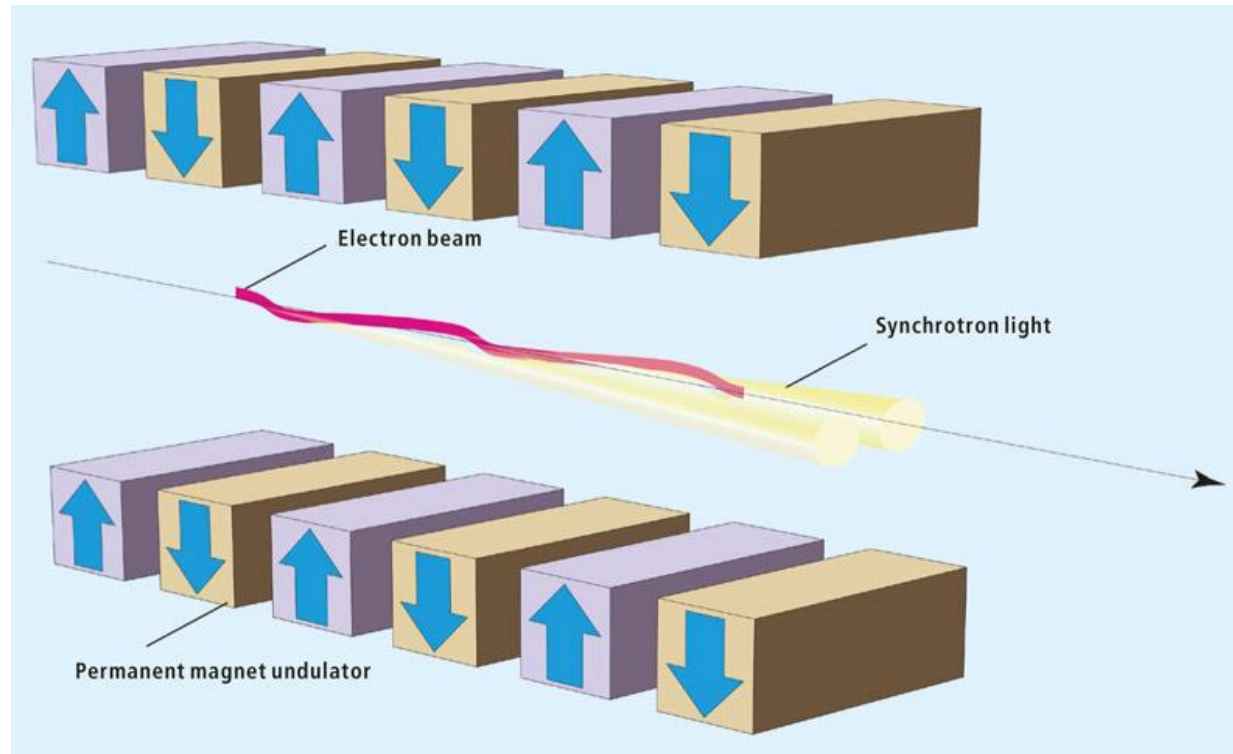


Outline

- **Undulator**
- **Undulator radiation**
- **Diagnostics examples**
 - **Emittance**
 - **Energy spread**
 - **Momentum compaction**
- **Conclusions**

Undulator

- Undulators are periodic structures made by sequences of dipole magnets and are used in synchrotron light sources to increase the flux produced in a narrow cone



<http://www.esrf.eu/Accelerators/news/art-undulator>

Undulator radiation

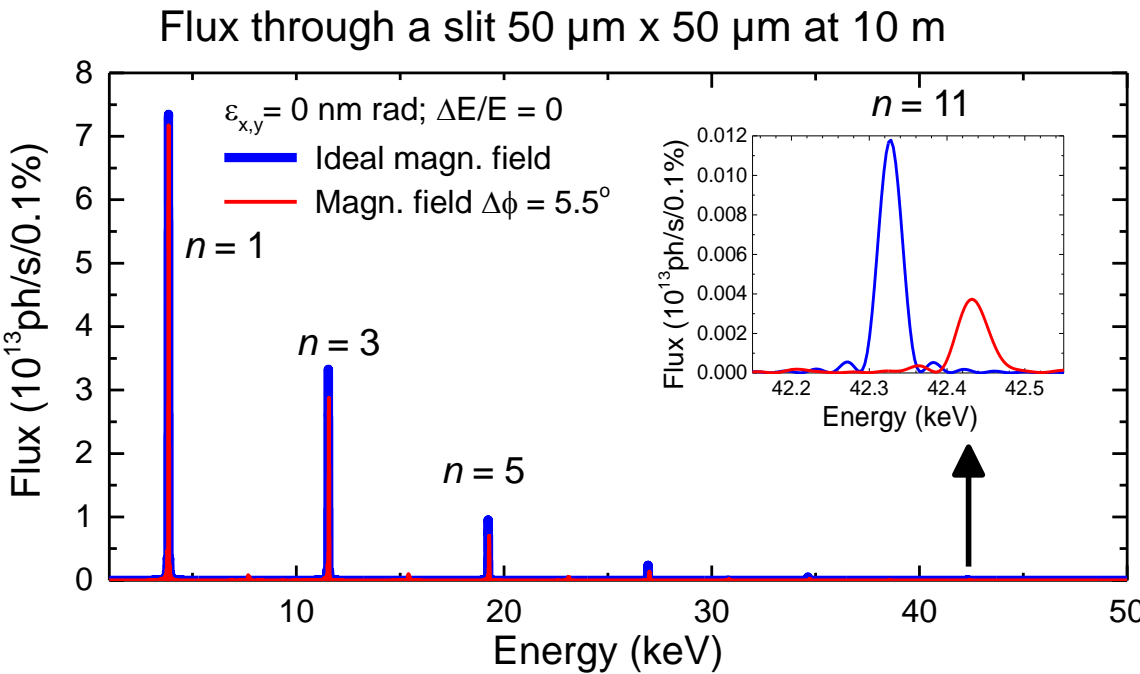
- The constructive interference of the radiation emitted at each pole gives rise to flux peaks at certain photon energies in the undulator spectrum: this can be used to qualify the undulator field quality as well as electron beam characteristics as emittance and energy spread.

$$\lambda = \frac{\lambda_U}{2 n \gamma^2} \left(1 + \frac{K^2}{2} + \gamma^2 \theta^2 \right)$$

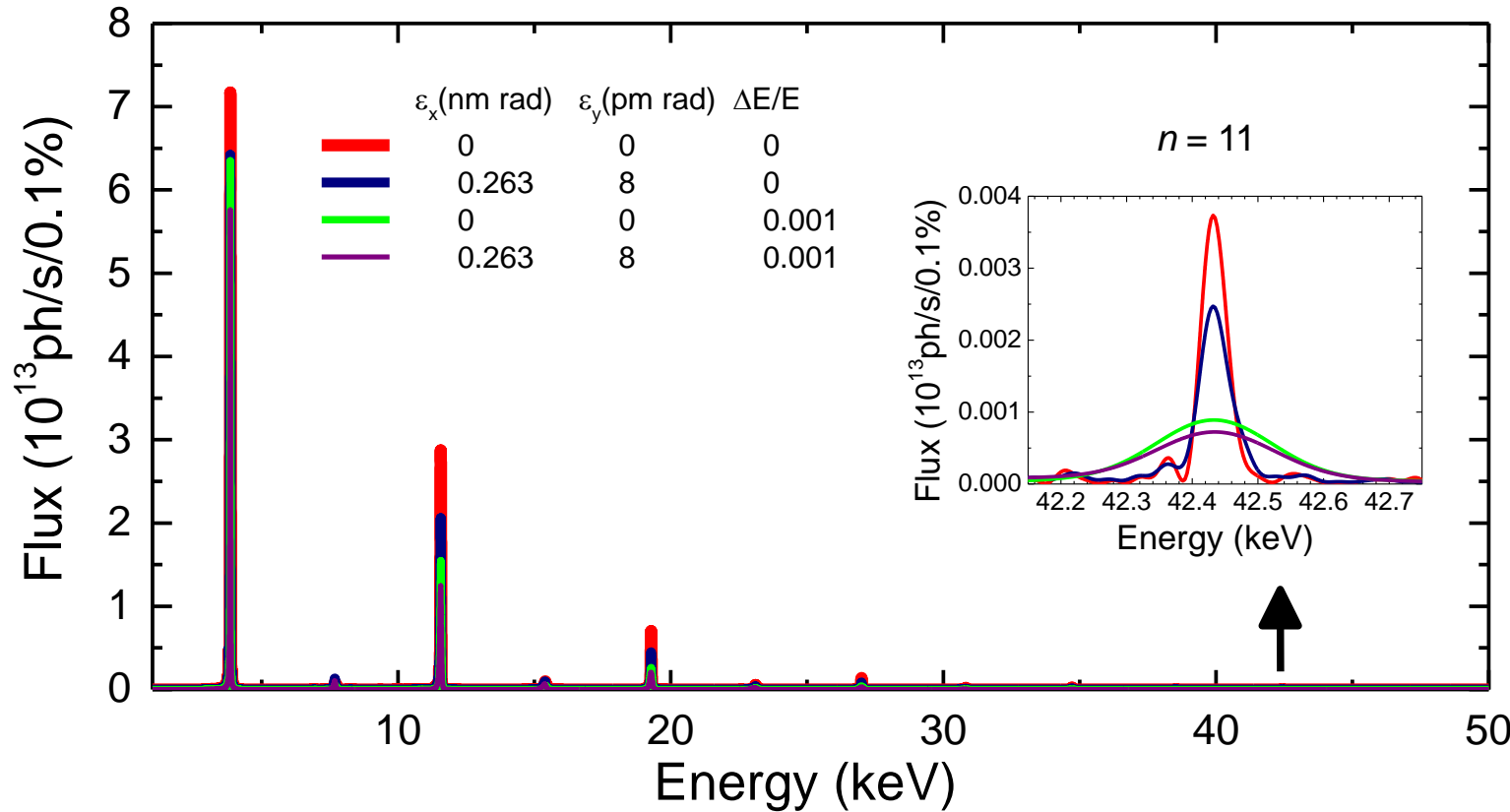
$$K = \frac{e}{2\pi m c} B_0 \quad \lambda_U = 0.9336 \ B_0 [T] \ \lambda_U [cm]$$

MAXIV parameters

E (Gev)	3
I (A)	0.5
$\Delta E/E$	0.001
ϵ_x (nm rad)	0.26
ϵ_y (nm rad)	0.008
β_x (m)	9
β_y (m)	4.8
η_x (m)	0
λ_U (mm)	15
B_{max} (T)	0.7
# full periods	102



Spectrum dependence on ϵ and $\Delta E/E$

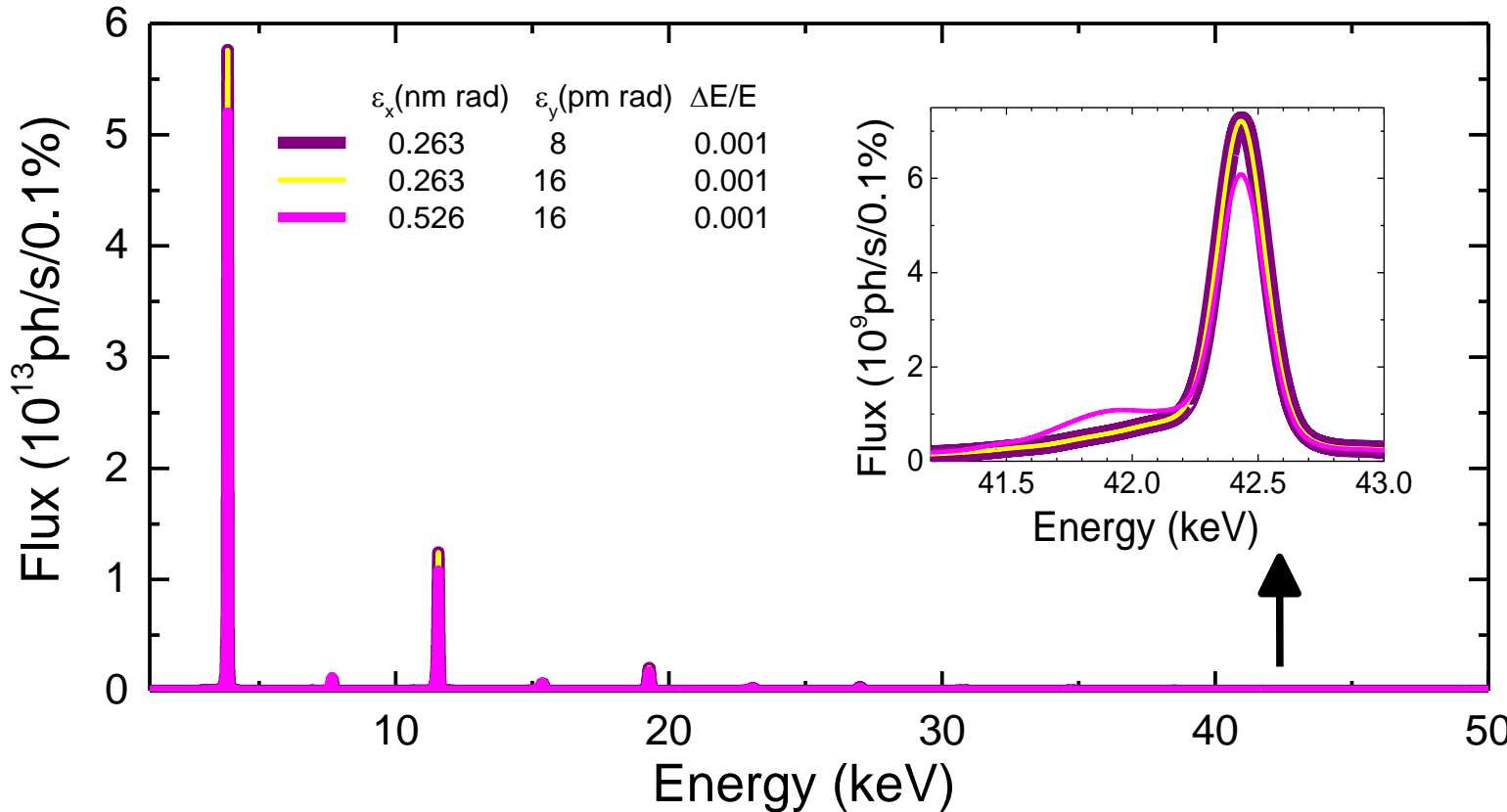


Largest suppression of higher harmonics from finite $\Delta E/E$
 Minimum value reached in storage rings $\Delta E/E \sim 0.001$

Simulations performed
 with SPECTRA[§]

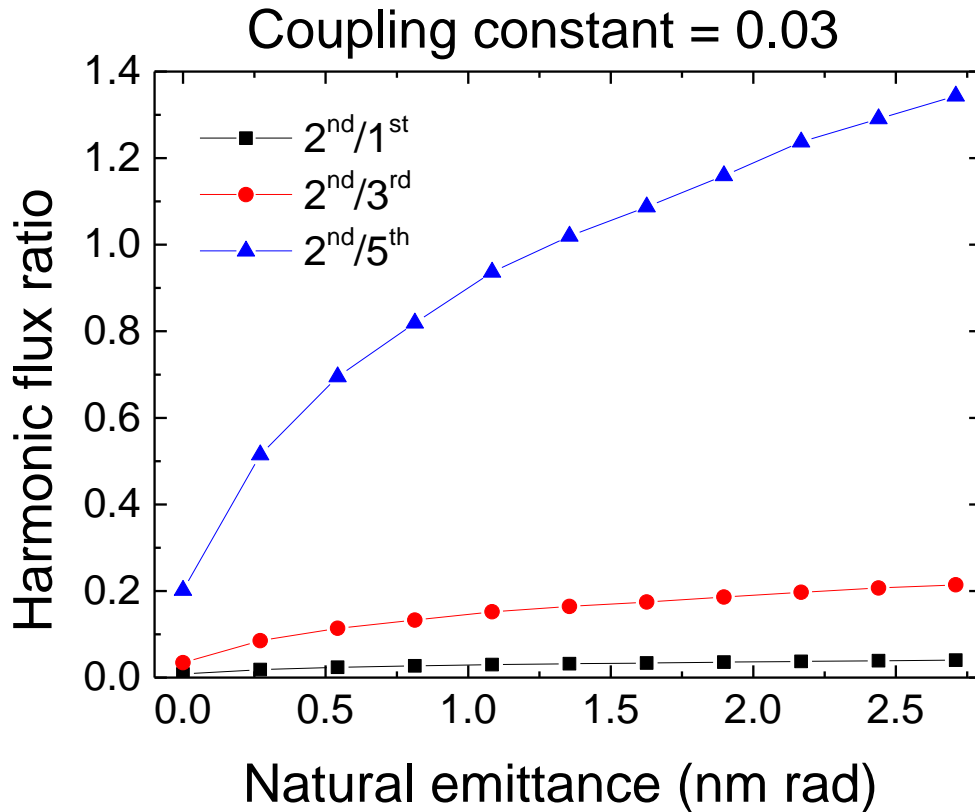
§T. Tanaka and H. Kitamura, J. Synchrotron Rad. 8, 1221 (2001)

Spectrum sensitivity to ϵ

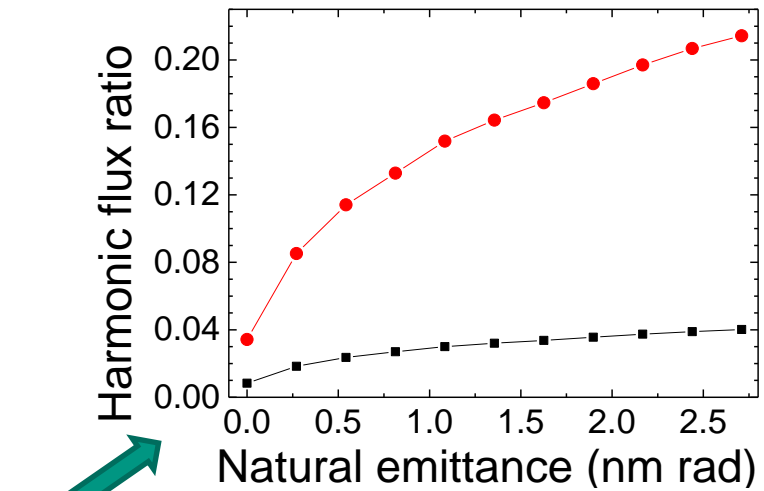


Increasing ϵ_y by a factor of 2 there is no change in the spectrum.
 Increasing ϵ_x by a factor of 2 the peaks decrease by about 20%.

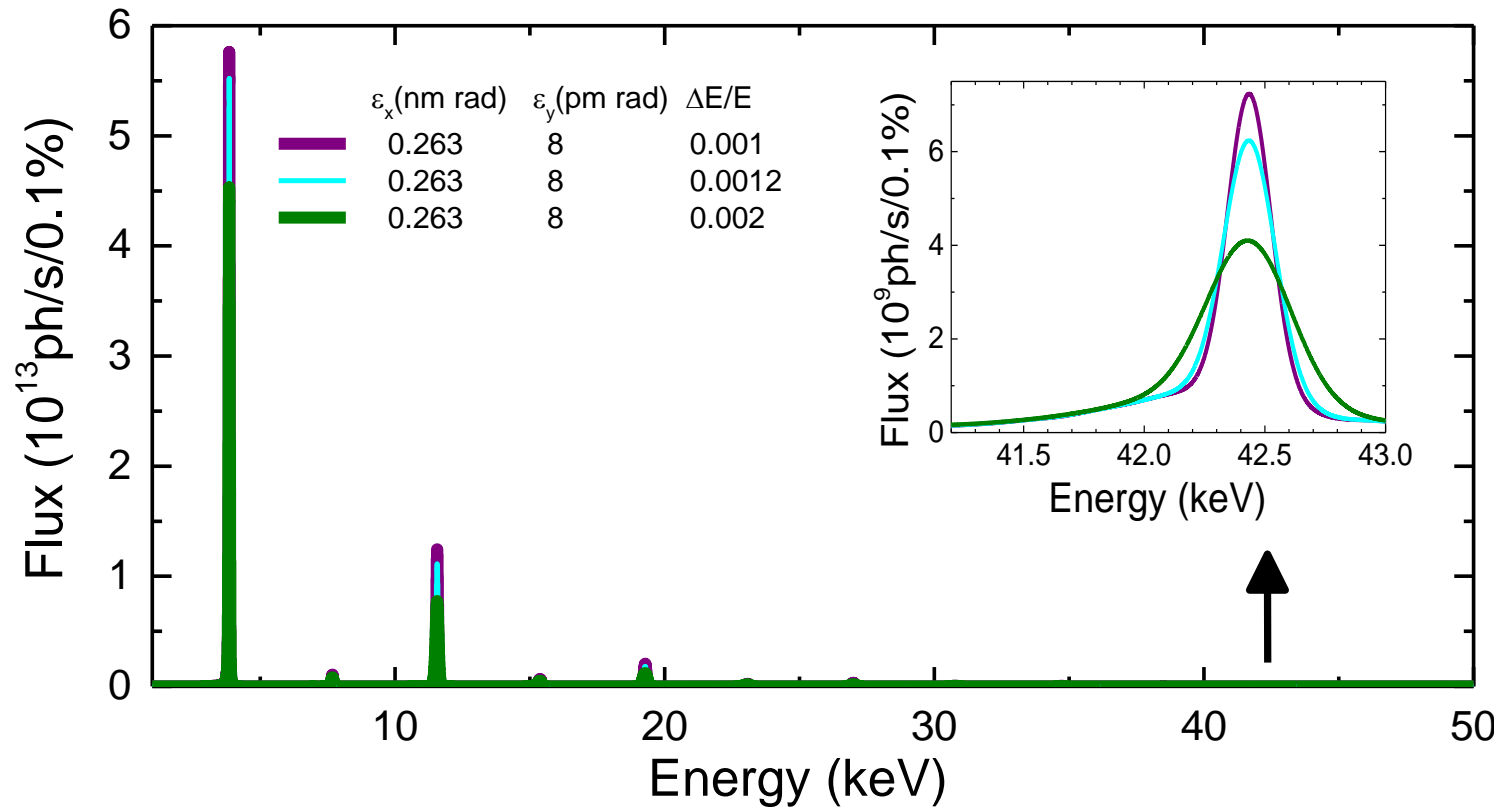
Spectrum sensitivity to ε : harmonic flux ratio



$$\frac{\Delta E}{E} = 0.1\%$$



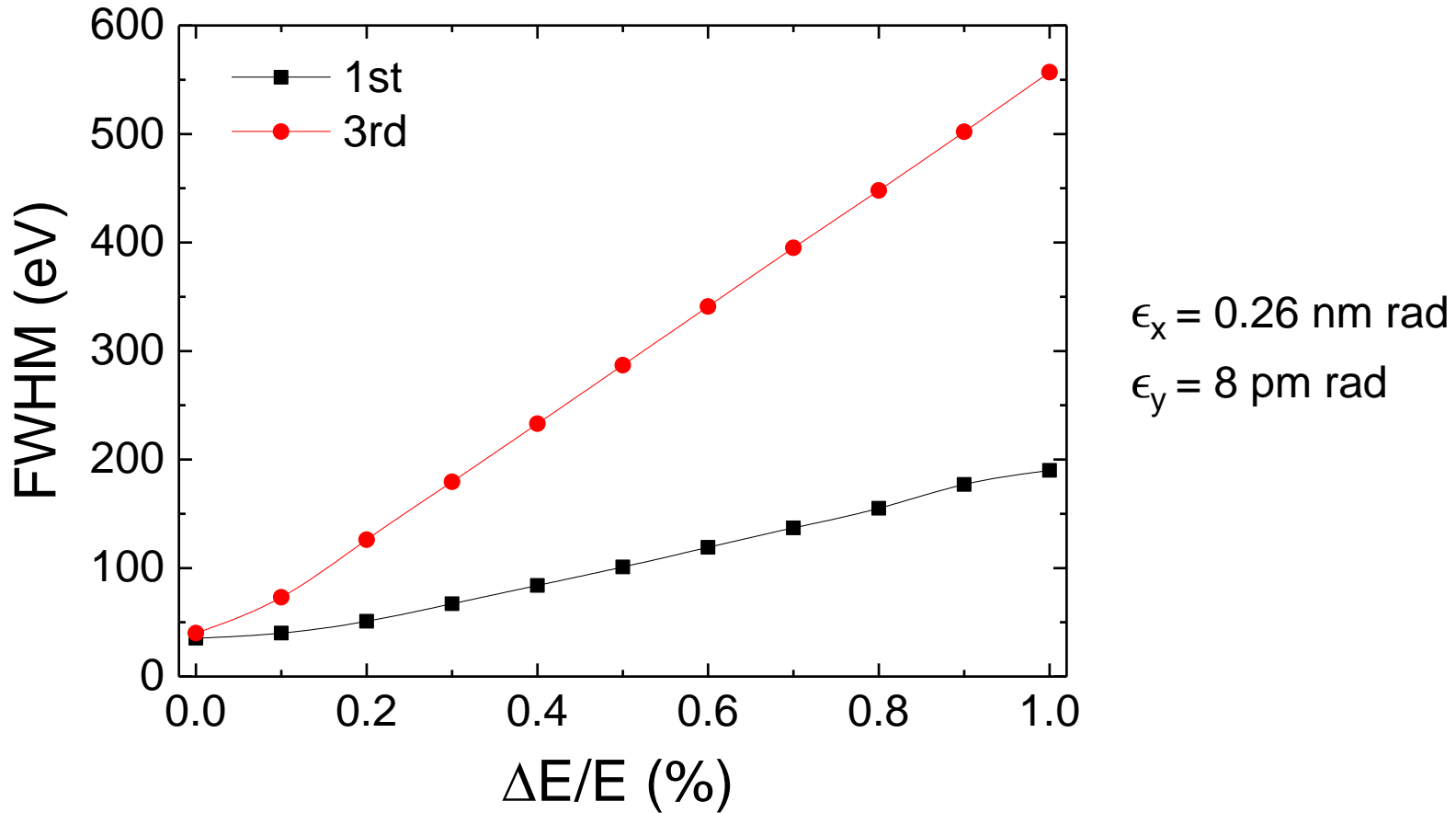
Spectrum sensitivity to $\Delta E/E$



Increasing $\Delta E/E$ by a factor of 2 there is 20% change in the height of the 1st harm. and about 50% in the height of the 11th.

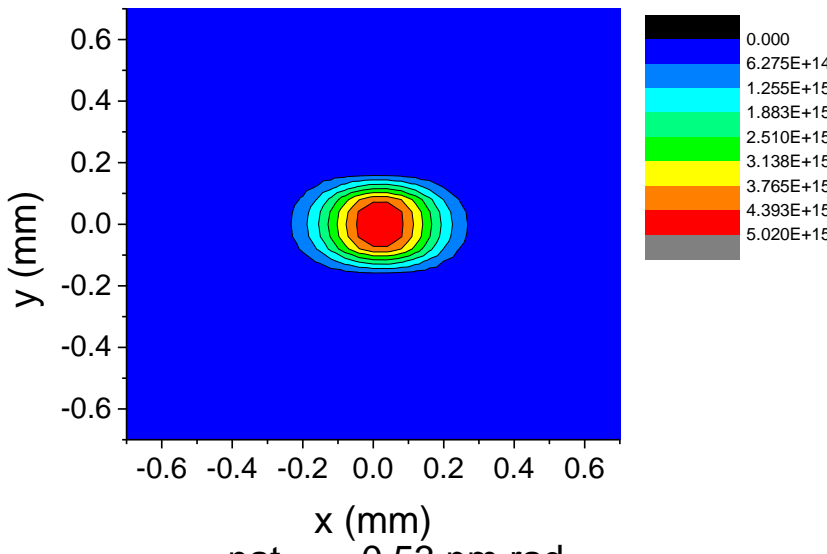
The higher harmonics are very sensitive to $\Delta E/E$ changes: 20% change in $\Delta E/E$ corresponds at the 11% harm. in a similar change in the peak height.

Spectrum sensitivity to $\Delta E/E$: line width

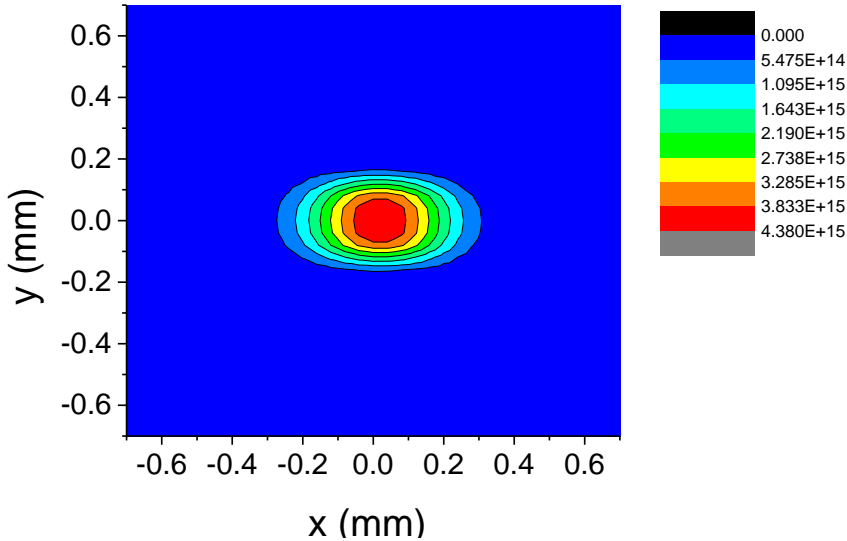


Harmonic spatial distribution

nat. $\varepsilon = 0.27 \text{ nm rad}$

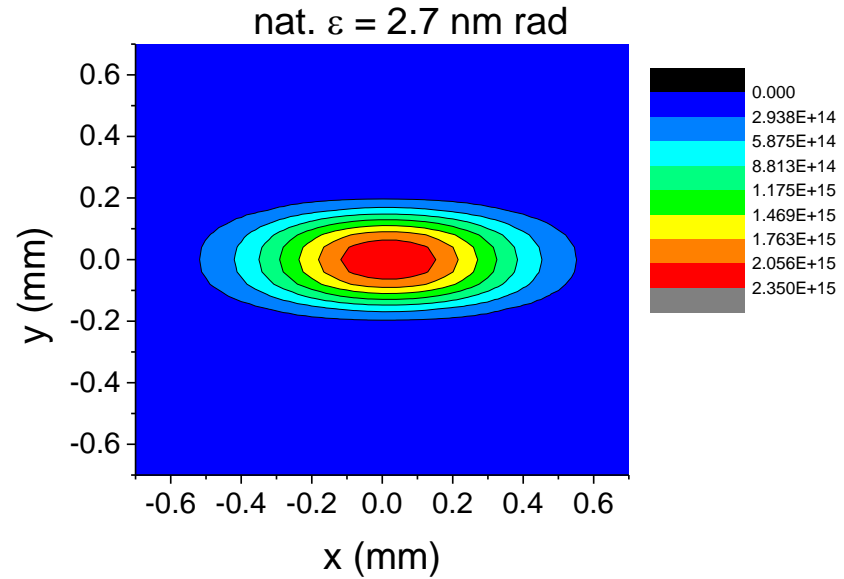


nat. $\varepsilon = 0.53 \text{ nm rad}$

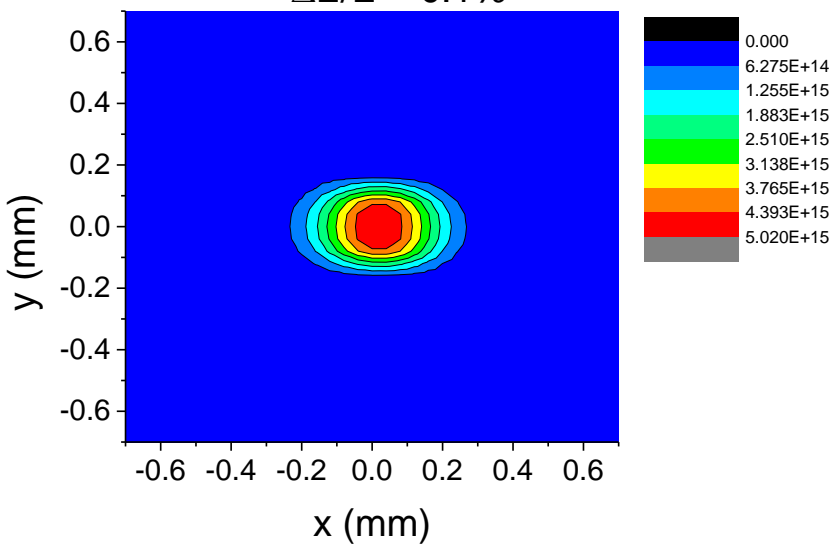


Coupling constant = 0.03

$$\frac{\Delta E}{E} = 0.1\%$$

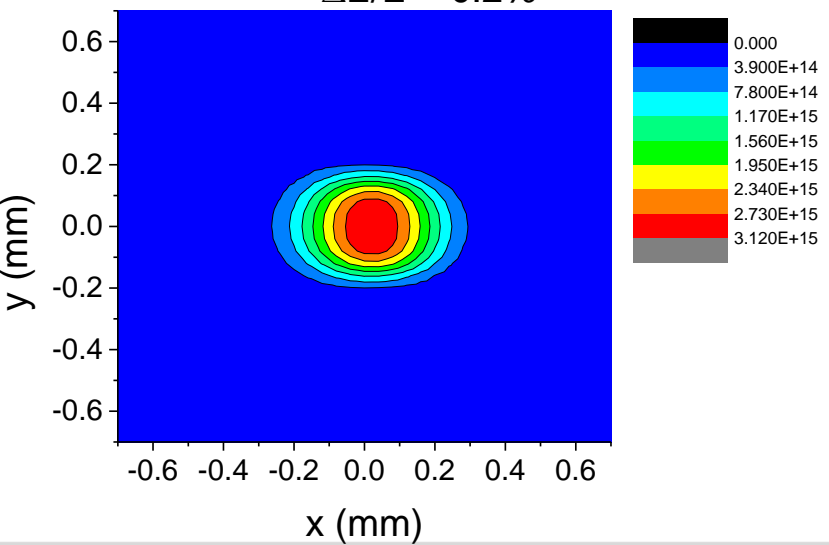
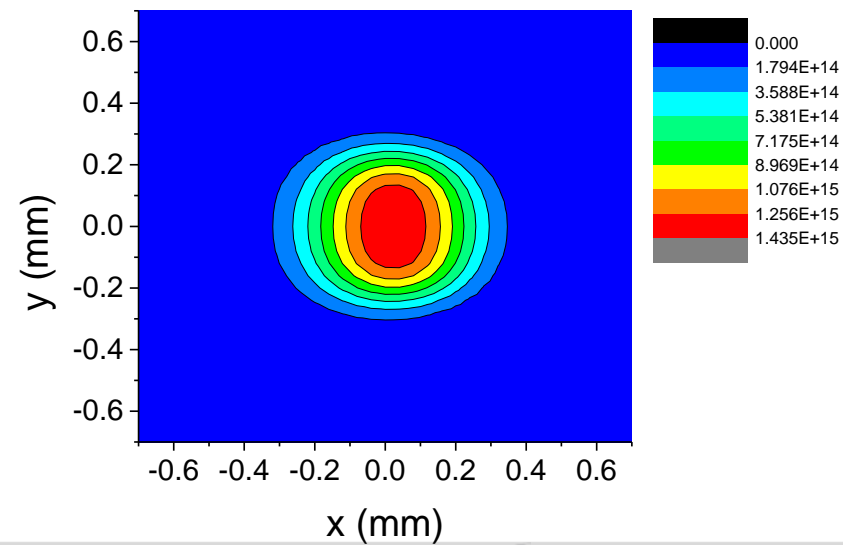


Harmonic spatial distribution

 $\Delta E/E = 0.1\%$


$\epsilon_x = 0.26 \text{ nm rad}$

$\epsilon_y = 8 \text{ pm rad}$

 $\Delta E/E = 0.2\%$

 $\Delta E/E = 0.5\%$


Examples

- Storage rings (SR): ESRF, APS
- Laser wakefield accelerator

SR: Emittance measurements

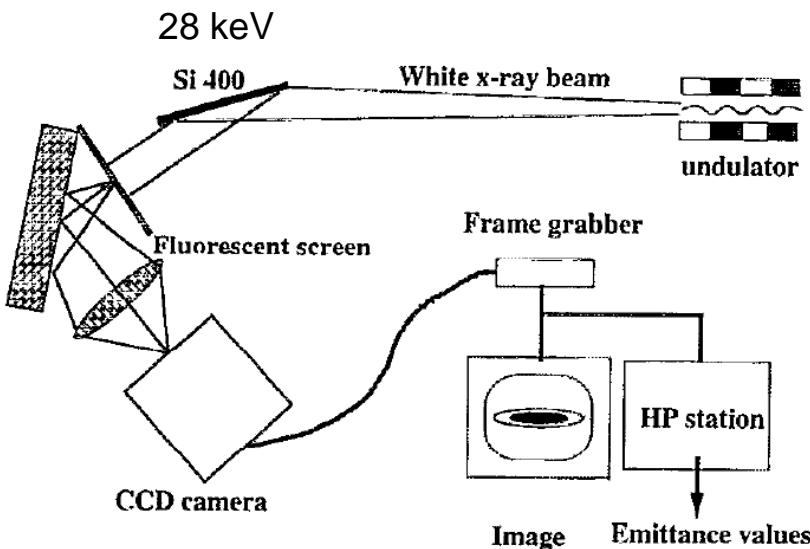


FIG. 1. Emittance monitor setup.

$$\epsilon = \frac{\sum_l^2 - \sigma_{\text{scr}}^2 - \sigma'_{\text{und}}^2 l^2}{\beta + l^2/\beta} \quad \sigma'_{\text{und}} = \sqrt{\frac{\lambda}{2L}}$$

Estimated error on $\epsilon \sim 20\%$

uncertainties in β functions and image quality (screen finite resolution $\sim 30 \mu\text{m}$)

E. Tarazona and P. Elleaume, Rev. Sci. Instr. 1974-1977 **66** (1995)

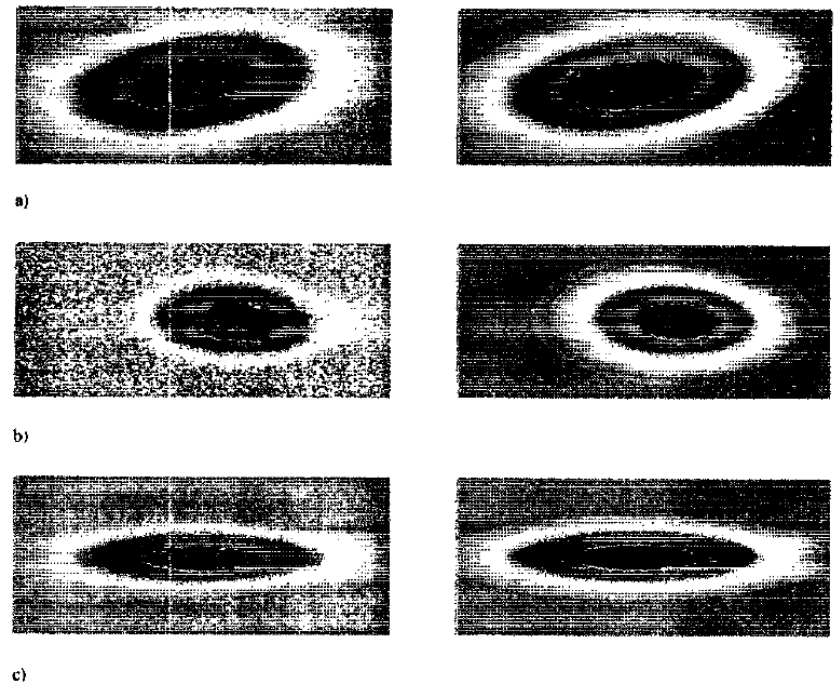


FIG. 2. Three different images of ID6 beam corresponding to different values of the emittance (on the left-hand side) and the fitted images (on the right-hand side). (a) $\epsilon_x = 10.6 \text{ nm}$, $\epsilon_z = 1.3 \text{ nm}$; (b) $\epsilon_x = 4.3 \text{ nm}$, $\epsilon_z = 0.55 \text{ nm}$; (c) $\epsilon_x = 10.3 \text{ nm}$, $\epsilon_z = 0.2 \text{ nm}$.

ESRF

SR: Energy and energy spread measurements

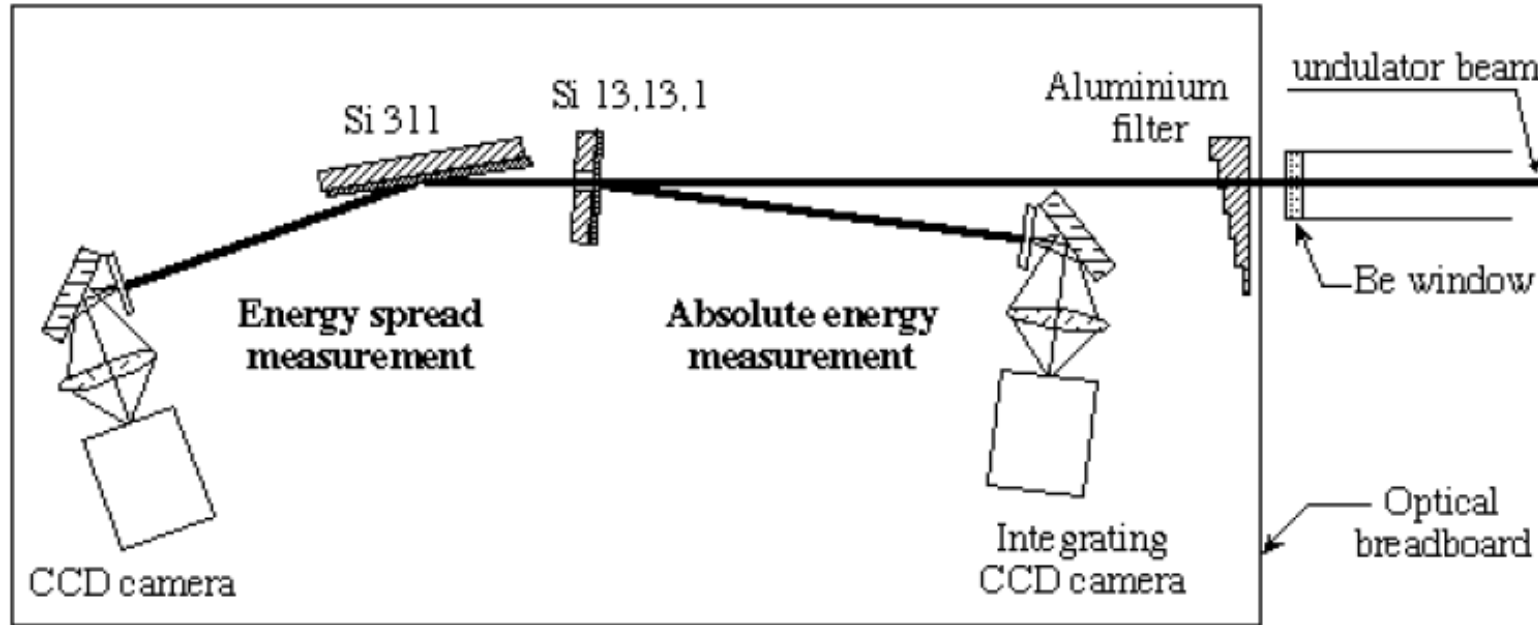


FIG. 1. Schematic of the electron average energy and energy spread measurement setups.

E. Tarazona and P. Elleaume, Rev. Sci. Instr. **67**, 3368 (1995)

ESRF

SR: Energy and energy spread measurements

Adjusting the magnetic gap, one makes the 3rd harmonic of the undulator coincide with the energy selected by the crystal

$$\lambda_n = \frac{1 + K^2/2}{2n(E/E_0)^2} \lambda_u \quad \frac{dE}{E} = \frac{dK}{K} \frac{K^2}{2 + K^2} < 0.1\%$$

Error on $\lambda_n \sim 0.0001$, minimized when $\theta \sim 90^\circ$ (Bragg law)

Error on $K \sim 0.01$

E. Tarazona and P. Elleaume, Rev. Sci. Instr. **67**, 3368 (1995)

SR: Energy and energy spread measurements

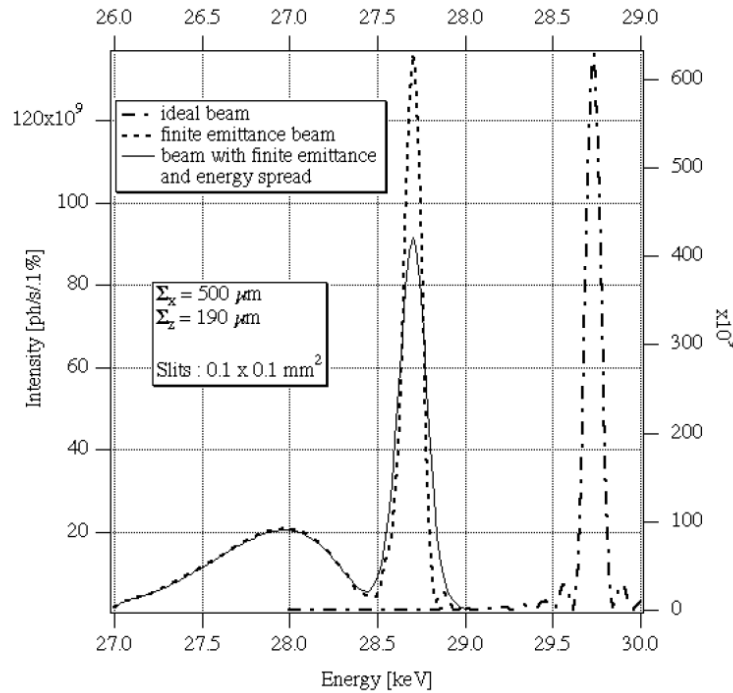


FIG. 2. Influence of the electron beam characteristics on the shape of the seventh harmonic. The case of a filament beam without energy spread is shown on the right curve (right and upper axes). The electron beam size and divergence are taken into account through the parameters Σ_x and Σ_z which are the horizontal and vertical sizes of the electron beam projected onto the slits. The effects of non-zero Σ_x , Σ_z (ie of a finite emittance beam) and energy spread are shown on the left curves.

E. Tarazona and P. Elleaume, Rev. Sci. Instr. **67**, 3368 (1995)

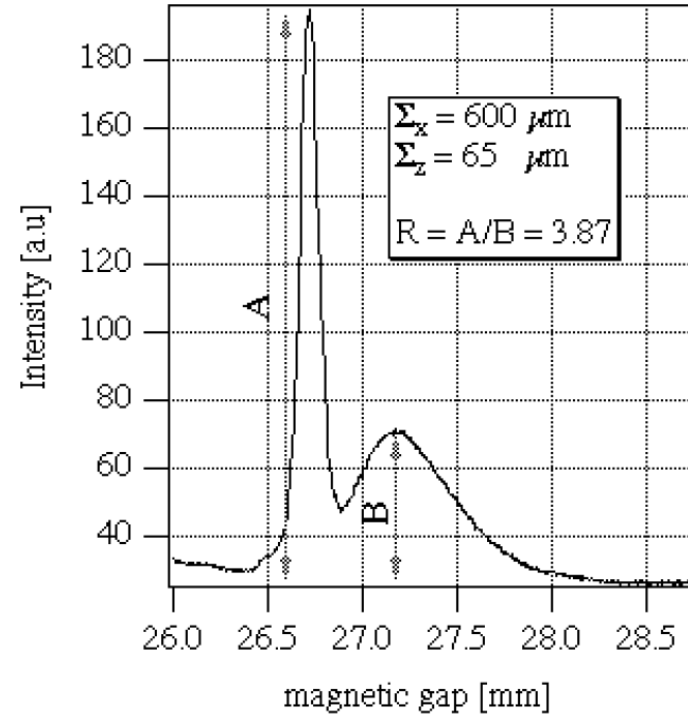


FIG. 4. Seventh harmonic profile recorded at a constant energy by varying the undulator gap. The energy spread deduced from Σ_x , Σ_z and R is 1.1×10^{-3} .

$$\frac{\Delta E}{E} = 0.0011 \pm 0.0002$$

SR: Momentum compaction factor

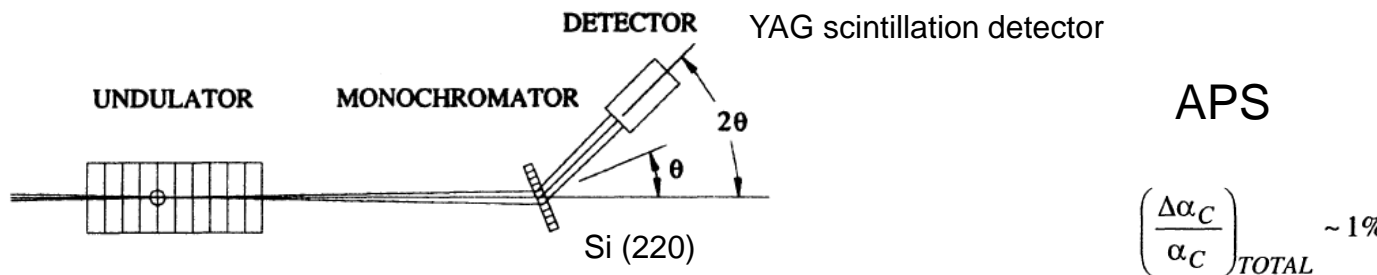


FIGURE 3. Schematic of the spectrum measurement of angle-integrated flux. The monochromator crystal uses Laue reflection with a Bragg angle θ , and the detector is located on a second rotary stage following 2θ .

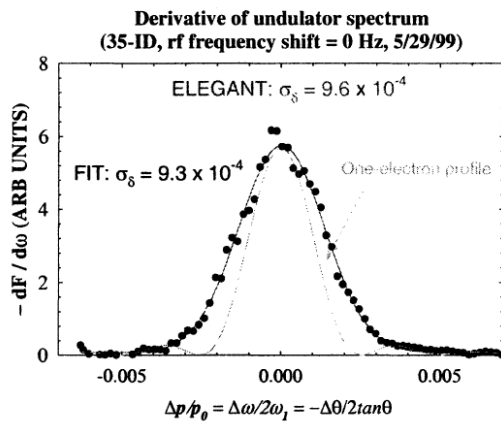


FIGURE 4. Scaled derivative spectrum of the total flux: (Dashed line) One electron radiation profile; (Circles) experimental measurements; and (Solid line) calculated value with electron energy spread assumed to be 0.93×10^{-3} .

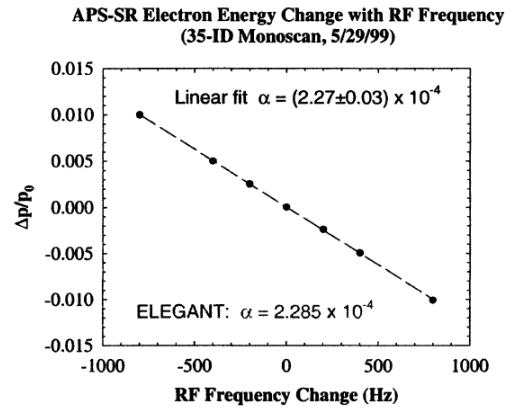
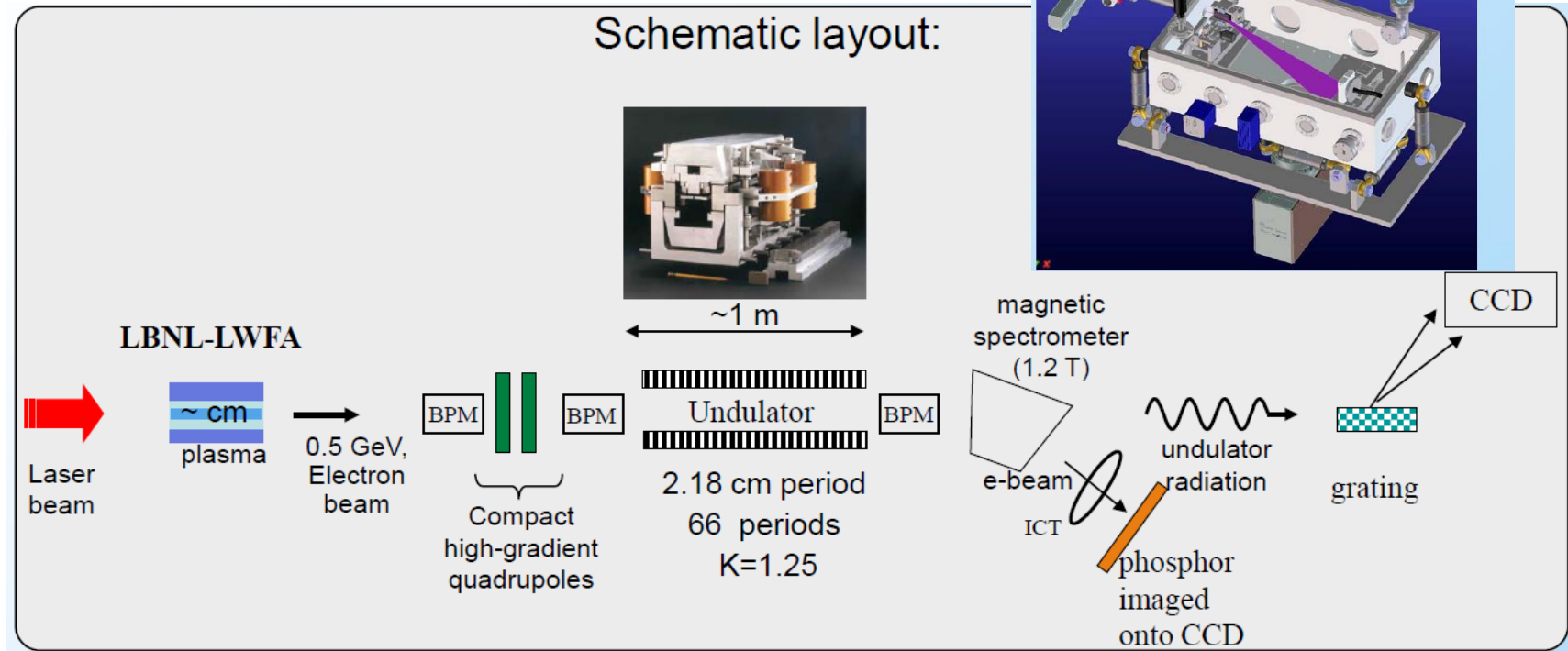


FIGURE 5. Energy centroid change as a function of rf frequency change. The slope of this curve gives the momentum compaction of the APS storage ring, 2.27×10^4 , compared with the simulation result of 2.285×10^4 .

B. Yang, M. Borland and L. Emery, Beam Instrumentation Workshop 2000

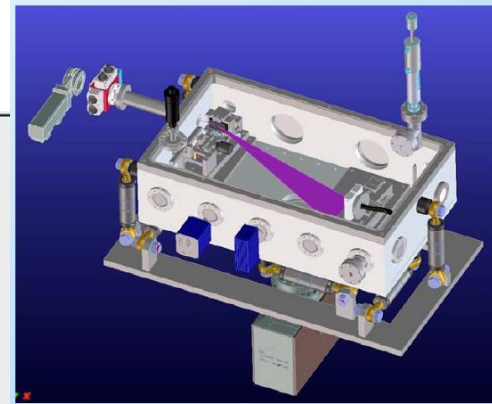
LWFA: Emittance and energy spread

M.S. Bakeman et al, FLS 2010

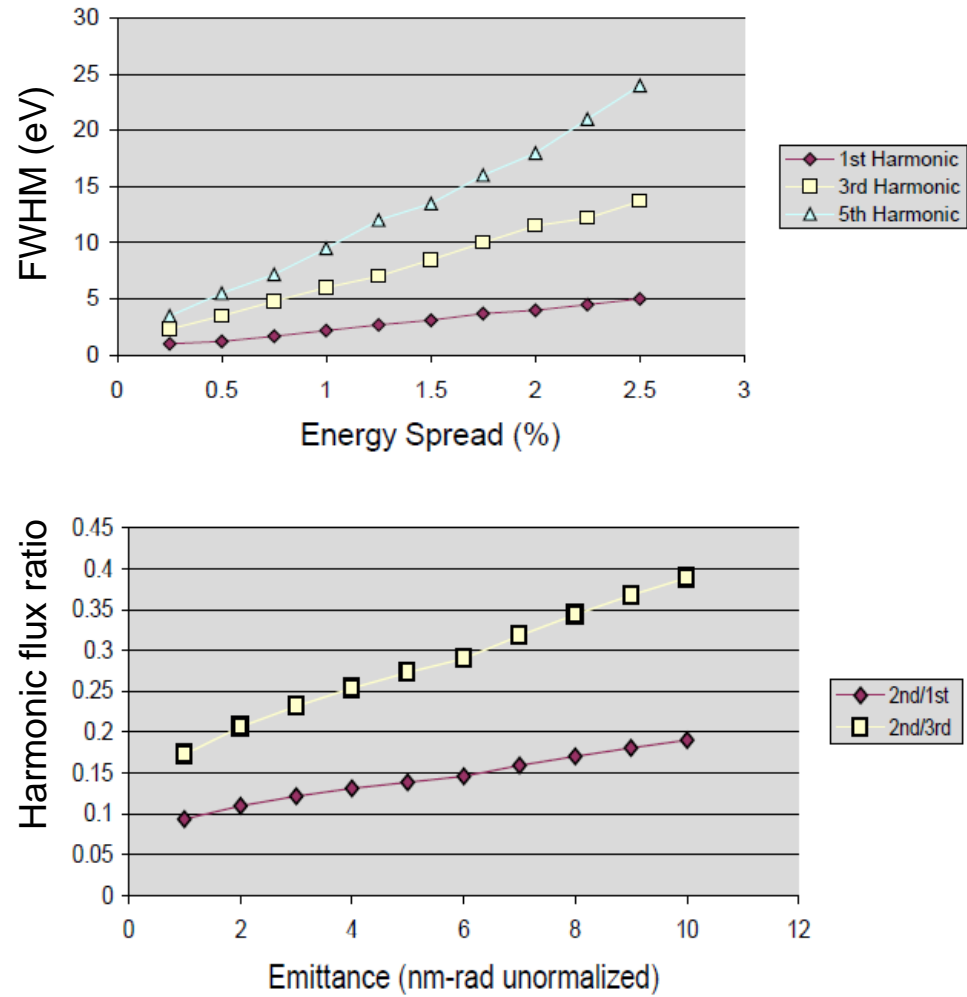
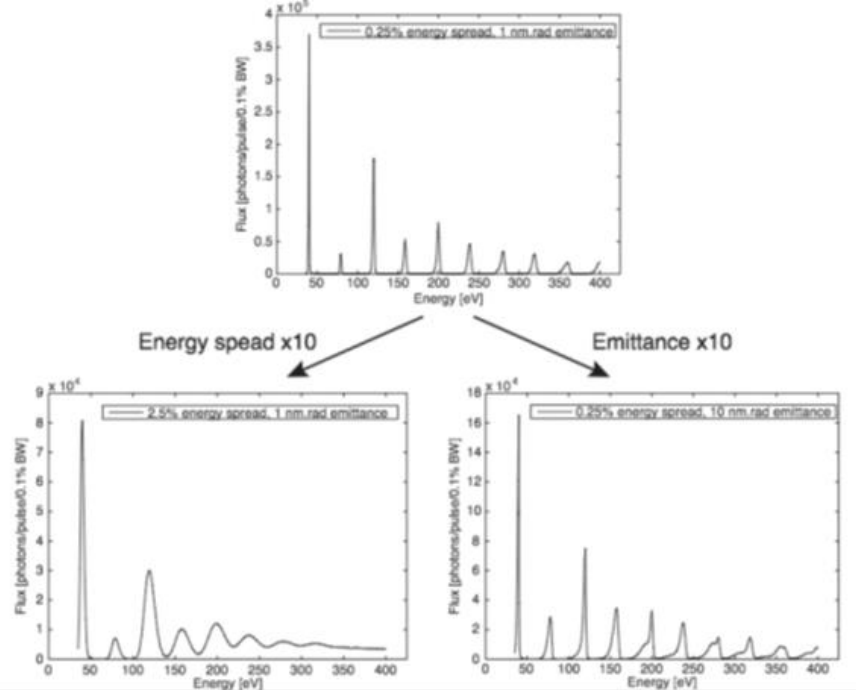


XUV Spectrometer properties

- 8-62nm spectral range
- Four jaw Aperture System
- MCP detector with CsI photocathode
- Aberration corrected concave grating



LWFA: Emittance and energy spread



M.S. Bakeman et al, FLS 2010

Conclusions

- Low emittance storage rings, free electron lasers and energy recovery linacs are designed to optimize the performance of the photons emitted by undulators
- Undulator radiation is a powerful diagnostic tool to measure emittance, energy spread and momentum compaction factor

Thanks to EUCARD² for providing the opportunity to attend this workshop

